Atmos. Chem. Phys. Discuss., 9, 1939–1975, 2009
www.atmos-chem-phys-discuss.net/9/1939/2009/

Atmospheric Chemistry and Physics Discussions

This discussion paper is/has been under review for the journal *Atmospheric Chemistry and Physics (ACP)*. Please refer to the corresponding final paper in *ACP* if available.

C_3-C_5 alkanes in the atmosphere: concentration, seasonal cycle and contribution to the atmospheric budgets of acetone and acetaldehyde

A. Pozzer[1,2], J. Pollmann[2], D. Taraborrelli[2], P. Jöckel[2], D. Helmig[3], P. Tans[4], J. Hueber[3], and J. Lelieveld[1,2]

[1]The Cyprus Institute, Energy, Environment and Water Research Center, P.O. Box 27456, 1645 Nicosia, Cyprus
[2]Air Chemistry Department, Max-Planck Institute of Chemistry, P.O. Box 3060, 55020 Mainz, Germany
[3]Institute of Arctic and Alpine Research (INSTAAR), University of Colorado, UCB 450, CO 80309, USA
[4]NOAA/ESRL, 325 Broadway, Boulder, CO 80303, USA

Received: 24 November 2008 – Accepted: 6 January 2009 – Published: 21 January 2009

Correspondence to: A. Pozzer (pozzer@cyi.ac.cy)

Published by Copernicus Publications on behalf of the European Geosciences Union.

Abstract

The atmospheric chemistry of C_3-C_5 alkanes has been incorporated in the atmospheric-chemistry general circulation model EMAC. Model output is compared with observations from the NOAA/ESRL GMD cooperative air sampling network. A new series of measurements is used to evaluate the model in representing C_3-C_5 alkanes (i.e. propane, isobutane, butane, isopentane and pentane). While the representation of propane is within the measurement standard deviation, some deviations are found for the other tracers. The model is able to reproduce the main features of the C_3-C_5 alkanes (e.g., seasonality). However, in the Northern Hemisphere during winter the mixing ratios of these alkanes are generally overestimated. Conversely, the model shows an underestimation in the Southern Hemisphere. Moreover, only for iso-pentane there is a net overestimation of the mixing ratios, while for the other alkanes, the results are at the higher end of the measurement range.

The effects of the C_3-C_5 alkanes to atmospheric acetone and acetaldehyde are quantified. The total amount of acetone produced by propane, isobutane and isopentane oxidation is 11.6 Tg/yr, 4.2 Tg/yr and 5.8 Tg/yr, respectively. These chemical sources are largely controlled by the reaction with OH, while the reactions with NO_3 and Cl contribute only to a little extent.

Moreover, 3.1, 4.5, 1.9 and 6.7 Tg/yr of acetaldehyde are formed from the oxidation of propane, butane, pentane and isopentane, respectively. Also for acetaldehyde, the formation is controlled by the reaction of alkanes with OH. However, since isopentane is generally overestimated, its contribution to the production of these oxygenated compounds represents an upper limit.

1 Introduction

Non Methane Hydrocarbons (NMHC) play an important role in tropospheric chemistry and ozone formation. They significantly influence the hydroxyl radical HO_x (=OH+HO_2)

budget through many complex reaction cycles (Logan, 1985; Houweling et al., 1998; Seinfeld and Pandis, 1997; Atkinson, 2000). For example, the NMHC are precursors to the formation of oxygenated organic compounds (OVOCs) such as acetone, formaldehyde and acetaldehyde. The seasonal and spatial distribution of NMHC is influenced by:

- emission strength (Singh et al., 2001, 2003; Singh and Zimmermann, 1992),
- photochemical reactions (Cardelino and Chameides, 1990; Singh et al., 1995; Neeb, 2000),
- atmospheric transport (Rood, 1987; Brunner et al., 2003),
- dilution due to atmospheric mixing of air (Roberts et al., 1985; Parrish et al., 2007).

Three-dimensional (3-D) global models which represent both transport and chemical processes are required to study and/or predict the spatial distribution and the temporal development of these species (Gupta et al., 1998; Roelofs and Lelieveld, 2000; Poisson et al., 2000; von Kuhlmann et al., 2003; Folberth et al., 2006). Here we compare results of the model EMAC model (ECHAM5/MESSy1 Atmospheric Chemistry) with data based on flask measurements (see Sect. 2.2) collected at remote locations across the globe during the years 2005–2006. The NHMC flask measurements (Pollmann et al., 2008) include quantification of ethane (C_2H_4), propane (C_3H_8), butane (or n-butane, C_4H_{10}), isobutane (or i-butane, I-C_4H_{10}), pentane (or n-pentane, C_5H_{12}) and isopentane (or i-pentane, I-C_5H_{12}). After a description of the model setup and the observational data set (Sect. 2), we present a comparison of the model results with the observations, focusing on propane and the isomers of butane and pentane. Finally, we discuss the contribution of C_3-C_5 alkanes to the atmospheric production and mixing ratios of the most important OVOC (Sect. 2.9), with a focus on the acetone budget.

2 Model and observations

2.1 Model description and setup

EMAC is a combination of the general circulation model ECHAM5 (Roeckner et al., 2006) (version 5.3.01) and the Modular Earth Submodel System (MESSy, version 1.1). The implementation follows the MESSy standard (Jöckel et al., 2005). A first description and evaluation of the model system was recently published (Jöckel et al., 2006; Pozzer et al., 2007). More details about the model system can be found at http://www.messy-interface.org. The model version used in this study is ECHAM5/MESSy1, and the setup is based on that of the evaluation simulation S1, as described by Jöckel et al. (2006). The setup was modified by adding the emissions of butane and pentane isomers, and their corresponding oxidation pathways (see Sect. 2.1.1 and Sect. 2.1.2). The simulation period covers the years 2005–2006, plus two additional months of spin-up time. The initial conditions are taken from the evaluation simulation of the model, here denoted as S1. Dry and wet deposition processes were extensively described by Kerkweg et al. (2006a) and Tost et al. (2006), respectively, while the tracer emissions were described by Kerkweg et al. (2006b). As in the simulation S1, the horizontal resolution adopted for the ECHAM5 base model is T42 ($\approx 2.8^\circ \times 2.8^\circ$). The applied vertical resolution is 90 layers, of which about 25 are located in the troposphere. The model setup includes feedbacks between chemistry and dynamics via radiation calculations. The model dynamics was weakly nudged (Jeuken et al., 1996; Jöckel et al., 2006; Lelieveld et al., 2007) towards the analysis data of the ECMWF (European Center Medium-range Weater Forecast) operational model (up to 100 hPa) in order to realistically represent tropospheric meteorology. This allows the direct comparison of model results with observations.

2.1.1 Chemistry

The chemical kinetics within each grid-box is calculated with the submodel MECCA (Sander et al., 2005). The set of chemical equations solved by the Kinetic PreProcessor (KPP, Damian et al., 2002; Damian-Iordache, 1996) in this study is essentially the same as in Jöckel et al., 2006. However, the propane oxidation mechanism (which was already included in the original chemical mechanism) has been slightly changed and new reactions for the butane and pentane isomers have been added. The complete list of differences from the original chemical mechanism used in Jöckel et al. (2006) is presented in the electronic supplement: http://www.atmos-chem-phys-discuss.net/9/1939/2009/acpd-9-1939-2009-supplement.pdf. The new reactions are a reduction of the corresponding detailed Master Chemical Mechanism (MCM, Saunders et al., 2003). In order to keep the number of reactions as low as possible for 3-D global simulations, the first generation products of the reactions of butanes (i.e. n-butane plus i-butane), pentanes (i.e. n-pentane plus i-pentane) with OH, NO_3, and Cl were directly substituted with their final degradation products, namely formaldehyde, acetaldehyde and acetone. The substitution also included the production of corresponding amounts of a model peroxy radical (RO_2) which has generic properties representing the total number of RO_2 produced during the "instantaneous oxidation". This serves the purpose of taking into account the $NO \rightarrow NO_2$ conversions and the $HO_2 \rightarrow OH$ interconversions. It was assumed that the reactions with OH and NO_3 have the same product distribution. The Cl fields were fixed with mixing ratios taken from the work of Kerkweg et al. (2008a,b, and reference therein). Thus, both alkanes and Cl fields are simulated without the need of a computationally expensive chemical mechanism.

2.1.2 Emissions

As pointed out by Jobson et al. (1994) and Poisson et al. (2000), the seasonal change in the anthropogenic emissions of NMHC are thought to be small, due to their dependencies on relatively constant fossil fuel combustion and leakage from oil and natural

gas production (Middleton et al., 1990; Blake and Rowland, 1995; Friedrich and Obermeier, 1999). The most detailed global emission inventory available is EDGAR (Olivier et al., 1999, 1996; van Aardenne et al., 2001), Emission Database for Global Atmospheric Research, which was applied for the evaluation simulation of EMAC (Jöckel et al., 2006). In the evaluation simulation S1 of the model (Jöckel et al., 2006), the anthropogenic emissions were taken from the EDGAR database (version 3.2 "fast-track", van Aardenne et al., 2005) for the year 2000. In order to keep the model as close as possible to the evaluation simulation S1, the propane emissions were not changed, with an annual global emission of 12 Tg/yr, as reported in Pozzer et al. (2007). For consistency, the total butanes and pentanes emissions from EDGARv2.0 were used in this study, being 14.1 Tg/yr and 12.4 Tg/yr, respectively (see Table 1). The speciation factors calculated by Saito et al. (2000) and Goldan et al. (2000), also used by Jacob et al. (2002), were used to obtain total emissions of 9.87 Tg/yr for n-butane (70% of butanes), 4.23 Tg/yr for i-butane (30% of butanes), 4.34 Tg/yr for n-pentane (35% of pentanes) and 8.06 Tg/yr for i-pentane (65% of pentanes), respectively. These fractions are still under debate: McLaren et al. (1996), for instance, showed that the ratio of n-pentane to i-pentane is 0.5. However, a ratio of 0.65 was preferred here, according to the extensive measurements of Saito et al. (2000). It must be stressed that the EDGAR database was criticized for the C_3-C_5 alkanes emission. As pointed out by Jacob et al. (2002), "...the EDGAR inventory underestimates considerably the observed atmospheric concentration of propane and i-butane over Europe, over the United States and downwind Asia". Based on these considerations, they suggested another emission inventory, as described by Bey et al. (2001), with a total i-butane and i-pentane emission of 3.6 Tg C/yr and 5.0 Tg C/yr, respectively. Gautrois et al. (2003), using measurements collected in Alert (Canada) and the Irvine Chemical Tracer Model (CTM, Prather et al., 1987), obtained a global emission of 22.7 Tg/yr for butanes and 8.2 Tg/yr for n-pentane. A few NMHC sources exist in remote locations in addition to emissions from urban and industrial regions. Biomass burning is a large source of propane, but a negligible source of butane and pentane isomers (Andreae and Merlet, 2001; Guenther et al., 2000). Bio-

genic sources of C_3-C_5 alkanes also appear to be negligibly small (Kesselmeier and Staudt, 1999). Other measurements in rural environments (Jobson et al., 1994; Goldan et al., 1995) show no evidence of biogenic emissions of saturated C_3-C_5 NMHC. Alkanes are also emitted by the oceans. Plass-Dülmer et al. (1995), estimated 1 Tg/yr as upper limit of the global emission for C_2-C_4 alkanes: 0.54 Tg/yr of ethane, 0.35 Tg/yr for propane and 0.11 Tg/yr of butanes. Broadgate et al. (1997) extrapolated global oceanic emissions of 0.03 Tg C/yr for i-butane and 0.14 Tg C/yr for n-butane, 0.03 Tg C/yr for i-pentane and 0.05 Tg C/yr for n-pentane. While oceanic propane emissions were included in this study, oceanic emission of higher alkanes were neglected due to their negligible impact and largely unknown spatio-temporal distribution.

2.2 Observations

The NOAA, ESRL, GMD (National Oceanic and Atmospheric Administration, Earth System Research Laboratory, Global Monitoring Division, Boulder, CO, USA) cooperative air sampling network currently consists of 59 active surface sampling stations, where usually one pair of flask samples is collected every week. This network is the most extensive global flask sampling network in operation, both in terms of number ofsites and total number of samples collected. Volatile Organic Carbons (VOC) data are available from approximately 40 of these sampling stations (see http://www.esrl.noaa.gov/gmd/), covering the latitudes from 82° N (ALT, Alert, Canada) to 89.98° S (SPO, South Pole station). Air samples are typically taken during predefined clean air periods, i.e., from specific wind directions only. A detailed description of the flask instrument and a full evaluation of the analytical technique was previously published (Pollmann et al., 2008). In summary, a custom-made sample extraction and inlet system interfaced to a gas chromatography – flame ionization detection (GC-FID) instrument was specially designed for the requirements of VOC measurements. The measurement system is typically calibrated 4 times a day each with an hydrocarbon standard and VOC free synthetic air. The instrument is fully automated and capable of quantifying up to 140 flask samples per week. An intercomparison with

the WMO, GAW (World Meteorological Organization, Global Atmospheric Watch) station in Hohenpeissenberg, Germany showed that these measurements meet the WMO data quality objective (World Meteorological Organization, 2007). These findings were confirmed during a recent audit by the World Calibration Center for Volatile Organic Compound (WCC-VOC, http://imk-ifu.fzk.de/wcc-voc/).

2.3 Overall model results

As explained in Sect. 1 and also confirmed by measurements (Gautrois et al., 2003; Lee et al., 2006; Swanson et al., 2003), the seasonal cycle of NMHC exhibits a maximum corresponding to the local winter and a minimum corresponding to the local summer. As shown by Hagerman et al. (1997) and Sharma et al. (2000), the seasonal cycle of C_2-C_5 alkanes is anti-correlated to the production rate of the main atmospheric oxidant (OH, see Spivakovsky et al., 2000; Jöckel et al., 2006). The flask measurements used in this study confirm this expected behavior and the model is able to reproduce the observed seasonal signal, with high mixing ratios during the local winter and low mixing ratios during the local summer. Contrary to Jacob et al. (2002), no underestimation of propane and i-butane mixing ratios was observed. Instead, while the model agrees well with the measurements for propane the model seems to overestimate the observed mixing ratios for the other tracers at most of the locations analyzed. The simulated mixing ratios for C_4H_{10}, I-C_4H_{10} and C_5H_{12} are at the high end of the measurement range, and only for I-C_5H_{12} there is a significant overestimation. Since the chemistry of C_3-C_5 is reasonably well understood, the errors in the estimations of their mixing ratios are strongly influenced by uncertainties in the emissions strength. The model, in fact, reproduces reasonably the atmospheric transport and dilution, as confirmed by the simulation of propane. In this case, because the emissions of propane are well constrained, its simulation reproduces the observations throughout the year at almost all latitudes (see Sect. 2.4). Hence, in this study, the emissions are the highest uncertainties between the processes influencing C_3-C_5 chemistry.

2.4 Propane, C_3H_8

As also shown in a previous analysis (Pozzer et al., 2007), the model simulation reproduces the main features observed for propane. The amplitude and phase of the simulated seasonal cycle also agree well with this new data set. As shown in Fig. 1, the seasonal cycle is well reproduced at the northern hemispheric sites (for example Alert, Canada (ALT) and Barrow, Alaska,BRW) which represent background conditions. Moreover, Fig. 2 shows that not only the seasonal cycle is correctly reproduced, but also the latitudinal gradients. As already mentioned by Swanson et al. (2003) and Bey et al. (2001), the original emission of 8.3 Tg/yr for propane proposed by the EDGAR database had to be increased to ∼11 Tg/yr. Nevertheless, the simulated mixing ratios are still slightly lower compared to the range of observations, and a further increase of the emissions may be needed in order to reproduce the measurements. Jacob et al. (2002) suggested a total source of 13.46 Tg/yr, although with a different spatial distribution. In this study the total emission of C_3H_8 are of ∼12 Tg/yr (see Sect. 2.1.2). In the Southern Hemisphere (SH) the model results seem to be somewhat lower than the observations in winter (January and February) and higher in summer (June, July and August). Interestingly, the model simulates a winter peak (July–August) at ∼30° S in the SH, which is not confirmed by the observations, due to the lack of sampling stations at this latitude. To confirm such a peak, we compared the model data with the PEM-Tropics-A (performed in SH Spring, Schultz et al., 1999, 2000) and PEM-Tropics-B (performed in SH Autumn, Raper et al., 2001a,b) campaign data from the Fiji region, using the database compiled by Emmons et al. (2000). As show in Fig. 3, the model tends to overestimate the mixing ratios of propane at the surface, probably due to too strong emission from the ocean. The bias appears during both winter and autumn of the SH. Although no final conclusion can be drawn due to the low density of continuous measurements in this region of the globe, it appears that the model is overestimating the concentration of propane throughout the year at those locations (30–40° S). Therefore we obtain no justification for a further increase of the emissions.

2.5 N-butane, C_4H_{10}

As mentioned in Sect. 2.3, the seasonal cycle of butane is correctly reproduced (Fig. 4). However, the winter peak seems to be overestimated in the Northern Hemisphere (NH). As observed by Blake et al. (2003) during the TOPSE campaign and also shown by the model, n-butane is removed quite rapidly at the onset of summer in all regions, and it is reduced to low levels (almost depleted) by late spring, except at the highest latitudes. A clear example is given in Fig. 4, for BRW, Barrow, Alaksa, where the modeled mixing ratios decrease from ∼400 pmol/mol in April to ∼1–2 pmol/mol in June and remain at this level during all NH summer (July and August). The observed latitudinal gradient is correctly simulated (see Fig. 5). The model simulates not only the correct gradient in the NH (within the standard deviations of the observations), but also the negative latitudinal gradient for latitudes higher than ∼75°, which is due to the low emissions in the remote Arctic region. A good agreement of the simulation with the observations is also achieved at Midway Island (Fig. 4, MID), a typical marine boundary layer (MBL) background station. Nevertheless the model underestimates the observed mixing ratios in NH winter at this location. This indicates that oceanic emissions could still play a role. A further analysis of the individual data rather than monthly averages will be needed to address this issue. In the SH, the model seems to underestimate the butane mixing ratios, with almost a total depletion during SH summer. While model simulates values below 1 pmol/mol during SH summer (December, January and February), the observations do not show the same behaviour, with summer values of ∼10 pmol/mol.

2.6 I-butane, I-C_4H_{10}

For i-butane the simulated mixing ratios are at the high end of the observed range for stations in the NH. However (see Fig. 6) the overestimation is less pronounced, and a better agreement (compared to to n-butane) between the simulation and the observations is achieved for most locations (for example in Cold Bay, USA, CBA). The latitudinal gradient is accurately simulated (see Fig. 7), although with a partial overestimation with

respect to the observations in the winter season for sites located in the industrialized regions (between 40° and 60° N). As for n-butane, in the SH the model seems to underestimate the observed mixing ratios (see Fig. 6, HBA, Halley Station, Antarctica). However, the measured data are close to the detection limit and the simulation is at the low end of the range of observations. As noticed in Sect. 2.3, the model does not underestimate the mixing ratios of i-butane in the USA and Europe, in contrast to the results obtained by Jacob et al. (2002). Opposite, the USA stations (see Fig. 6, LEF, Park Falls, USA) show an overestimations of the observed mixing ratios.

2.7 N-pentane, C_5H_{12}

The simulated mixing ratios of n-pentane agree with the observed values at most locations (see Fig. 8). In Alert, Canada (ALT) or Park Falls, USA (LEF), for example, the simulation reproduces not only the observed seasonal cycle (in magnitude and intensity), but also the variability of the measurements. In Fig. 8 the simulated and observed concentrations for n-pentane are presented for different locations. The model reproduces the phase of the seasonal cycle at all locations. Nevertheless, the simulated mixing ratios are lower than observed throughout all seasons in the subtropics and in the SH (Fig. 8, MID, Midway Island, USA and KUM, cape Kumukahi, USA). However, as mentioned before, the mixing ratios are close to the instrumental detection limits in these regions and the instrumental error could be relatively high. Nevertheless a bias between the model results and the observations is evident; the short lifetime of C_5H_{12} (shorter than the interhemispheric exchange time), indicates that the emissions are generally underestimated in the SH. This is corroborated by the same results of i-pentane, which has the same sources in this region (see also Sect. 2.8). The zonal gradient in winter confirms this conclusion (see Fig. 9). The NH mixing ratios are correctly simulated (within a factor of 2), while the mixing ratios in the SH are clearly underestimated.

2.8 I-pentane, I-C_5H_{12}

Despite the good representation of n-pentane, the simulated i-pentane mixing ratios are higher than the observations in the NH. The overestimation in NH remote regions (see Fig. 10, ALT, Alert,Canada) occur during the NH winter, with an overestimation of ∼200–300%. Nevertheless the simulated mixing ratios of i-pentane match the observations in the NH during May, June and July. This indicates a seasonality of the emissions. On the other hand, the model tends to underestimate the mixing ratios of I-C_5H_{12} in the NH subtropics and in the SH (see Fig. 10, MID, Midway Island, USA and KUM, cape Kumukahi, USA). As mentioned in Sect. 2.7, this points to a partially wrong distribution of the emission patterns, which are probably unbalanced and located almost exclusively in the NH, notably in the industrialized regions. This is also visible in Fig. 11. The latitudinal gradient is generally very steep and peaks in the industrialized regions, overestimated by a factor of 3 to 5.

2.9 Contributions to the atmospheric budget of some OVOCs

2.9.1 Acetone formation

Acetone (CH_3COCH_3), due to its photolysis, plays an important role in the upper tropospheric HO_x budget (Singh et al., 1995; McKeen et al., 1997; Müller and Brasseur, 1995; Wennberg et al., 1998; Jaeglé et al., 2001). Moreover, this trace gas is essential to correctly describe the ozone enhancement in flight corridors (Brühl et al., 2000; Folkins and Chatfield, 2000). The chemical formation of acetone by oxidation of propane and C_4-C_5 isoalkanes (Singh et al., 1994) has been estimated to be ∼22% of the total sources of acetone (Jacob et al., 2002).

The transport and chemical production of acetone were explicitly calculated with EMAC. Globally, the total production of acetone from C_3-C_5 alkanes is 21.6 Tg/yr. Propane decomposition produces ∼11.6 Tg/yr, with a yield of 0.73. On the other hand, the total production of acetone from C_4-C_5 isoalkanes oxidation is 10 Tg/yr. I-

butane oxidation produces 4.2 Tg/yr acetone, 91% of it in the NH (∼3.8 Tg/yr). At the same time 5.8 Tg/yr of acetone is produced by i-pentane oxidation, 91% of it in the NH (∼5.3 Tg/yr). The model calculation presented here indicates that CH_3COCH_3 is produced solely by the reaction of the iso-alkanes with OH; the contribution of the reaction with Cl and NO_3 are negligible, being less than 0.5% of the total. In their study, Jacob et al. (2002) calculated an acetone production of 14 Tg/yr, 4.0 Tg/yr and 2.6 Tg/yr from propane, i-butane and i-pentane, respectively. The differences compared to our estimates arise from the different emissions and acetone yield applied. For instance, Jacob et al. (2002) used 0.93 and 0.52 for i-butane and i-pentane (with OH), respectively. In this study, instead, acetone yields of ∼0.99 from i-butane and and ∼0.90 from i-pentane were obtained from the chemical mechanism. For propane, where the acetone yield is very similar (0.72) to the one obtain in this work (0.73), a difference in the emissions (13.46 Tg/yr vs. 12 Tg/yr see Table 1) causes a slight difference in the acetone production. In addition, reactions with Cl and NO_3 were added, although they do not play a significant role in the acetone chemistry. The results from this model study were compared to the evaluation simulation S1 (see Sect. 2.1). The S1 analysis did not account for NMHC with more than 4 carbons and their subsequent atmospheric reactions. This allows us to evaluate the effect of higher NMHC in global models. The consequent increase of the acetone mixing ratios is evident, especially in the NH. As shown in Fig. 12, the acetone mixing ratio increased at the surface by 300 pmol/mol in the remote NH regions (for example in the Pacific Ocean). The relative effect in polluted regions is smaller (maximum increase ∼30%) due to the already strong anthropogenic emission of acetone. However, the contributions from these alkanes are significant. The strong emissions of butanes and pentanes in the Persian Gulf region are due to fossil fuel production and petrochemical industry in the Middle East region and to a lesser extent in the Mediterranean region, and consequently transported to the Persian Gulf region (Lelieveld et al., 2002; Traub et al., 2003). In this region the maximum effect of C_4-C_5 alkanes on acetone is achieved, with an increase of its mixing ratio of ∼1000 pmol/mol, combined with an increase of ∼450 pmol/mol over the entire

Mediterranean region. The mixing ratio of acetone in the SH is practically not affected by chemical formation from iso-alkanes, simply because they are mainly emitted in the NH. This, combined with their short lifetime (shorter than the interhemispheric exchange time), confine the iso-alkanes to decompose and produce acetone only in the NH. To confirm the improvements in the acetone budget obtained including the C_4-C_5 alkanes, the model simulation was compared with some field campaign data reported by Emmons et al. (2000). As shown in Fig. 13, the inclusion of the C_4-C_5 alkanes chemistry substantially increased the concentration of acetone in the North Pacific region (PEM-Tropics-B and PEM-West-B). In these cases, the increase is ∼50% compared to a simulation without these alkanes. The simulated mixing ratios now agree much better with the measurements. Especially below 5 km altitude, the simulated vertical profiles are closer to the observations, being improved compared to the evaluation simulation S1. In a highly polluted region (TRACE-P, China, Fig. 13) downwind of China, the inclusion of C_4-C_5 compounds improves the simulation of acetone. The underestimation of the free-troposphere mixing ratios seems to support the revision of the acetone quantum yield, as proposed by Blitz et al. (2004). Arnold et al. (2005), in fact, calculated an average increase of ∼60–80% of acetone in the upper troposphere.

2.9.2 Acetaldehyde formation

Acetaldehyde (CH_3CHO) is also formed during the degradation of C_3-C_5 alkanes. This tracer is a short-lived compound, with an average lifetime of several hours (Tyndall et al., 1995, 2002). It is an important precursour of PAN (peroxyacetyl nitrate), a reservoir species for NO_x (see Singh et al., 1985; Moxim et al., 1996). In this study, with the use of the EMAC model, the calculated production of acetaldehyde from C_3-C_5 alkanes is 16.2 Tg/yr, 13.1 Tg/yr from the C_4-C_5 alkanes degradation. 3.1 Tg/yr, 4.5 Tg/yr, 1.9 Tg/yr and 6.7 Tg/yr of the acetaldehyde comes from the oxidation of propane (C_3H_8) butane (C_4H_{10}), pentane (C_5H_{12}) and i-pentane (I-C_5H_{12}), respectively. These amounts are solely produced by the reaction with OH; in fact, the reaction of C_3-C_5 alkanes with NO_3 produces only 0.1% of the total acetaldehyde. As for ace-

tone the production is largely confined to the NH (14.9 Tg/yr) and only 8% of the global production of acetaldehyde is located in the SH (1.3 Tg/yr).

3 Conclusions

We compared the EMAC model results of C_3-C_5 alkanes with observational data obtained from flask measurements from the NOAA/ESRL flask sampling network. Overall, the model reproduces most of the observations of propane, butanes and pentanes mixing ratios. The seasonal cycle is correctly reproduced, while the mixing ratios are within a factor of 3 compared to the observations. The simulation of propane (C_3H_8) shows good agreement with the observations, both with respect to the spatial and the temporal distribution. A peak at 30° S is observed during the southern hemispheric winter. The use of aircraft observation taken from Emmons et al. (2000) that partially cover this region in time and space did not confirm such feature in the propane spatio-temporal distribution. Generally, the simulated seasonal cycles of the butanes and pentanes agree well with the observations. Nevertheless, the simulated butanes mixing ratios are overestimated during the winter at the NH stations, being at the high end of the measurement range. Conversely, in the SH the simulation underestimates the observed mixing ratios. For n-pentane we achieve a good agreement between the NH observations and the simulated values. On the other hand, iso-pentane is generally overestimated at all locations. Additional studies will have to focus on the SH stations, where the butanes and pentanes mixing ratios are close to the detection limit of the instruments. A more detailed analysis of the instrumental error and comparison with model results is necessary before we can draw a firm conclusion regarding the ability of the model to represent these tracers in such remote areas. The inclusion of C_4-C_5 alkanes in the model improves the representation of acetone (CH_3COCH_3). Iso-butane and iso-pentane degradation produces ∼4.2 and ∼5.8 Tg/yr of acetone, respectively. The formation of acetaldehyde was also calculated, resulting in a production rate of 4.5 Tg/yr, 1.9 Tg/yr and 6.7 Tg/yr from the oxidation of n-butane, n-pentane and

i-pentane, respectively. Rememer that I-C_5H_{12} is generally overestimated. Hence, the contribution of i-pentane to the production of these oxygenated compounds represents an upper limit. The role of NO_3 and Cl in the degradation of C_3-C_5 isoalkanes and formation of acetone and acetaldehyde is negligible, contributing less than a few percent to the total chemical production.

Acknowledgements. The authors wish to acknowledge the use of the Ferret program for analysis and graphics in this paper. Ferret is a product of NOAA's Pacific Marine Environmental Laboratory (information is available at: http://www.ferret.noaa.gov). The authors acknowledge the efforts of all NOAA sampling personnel worldwide.

This Open Access Publication is
financed by the Max Planck Society.

References

Andreae, M. O. and Merlet, P.: Emission of trace gases and aerosols from biomass burning, Global Biogeochem. Cy., 15, 955–966, 2001.

Arnold, S. R., Chipperfield, M. P., and Blitz, M.: A three-dimensional model study of the effect of new temperature-dependent quantum yields for acetone photolysis, Geophys. Res. Lett., 110, D22305, doi:10.1029/2005JD005998, 2005.

Atkinson, R.: Atmospheric chemistry of VOCs and NO_x, Atmos. Environ., 34, 2063–2101, 2000.

Bey, I., Jacob, D. J., Yantosca, R. M., Logan, J. A., Field, B. D., Fiore, A. M., Li, Q., Liu, H. Y., Mickley, L. J., and Schultz, M. G.: Global modeling of tropospheric chemistry with assimilated meteorology: Model description and evaluation, J. Geophys. Res., 106, 23073–23095, 2001.

Blake, D. and Rowland, S.: Urban leakage of liquefied petroleum gas and its impact on Mexico City air quality, Science, 269, 953–956, 1995.

Blake, N. J., Blake, D. R., Sive, B. C., Katzenstein, A. S., Meinardi, S., Wingenter, O. W., Atlas, E. L., Flocke, F., Ridley, B. A., and Rowland, F. S.: The seasonal evolution of NMHCs and light alkyl nitrates at middle to high northern latitudes during TOPSE, J. Geophys. Res., 108(D4), 8359, doi:10.1029/2001JD001467, 2003.

Blitz, M., Heard, D., Pilling, M., Arnold, S. R., and Chipperfield, M. P.: Pressure and temperature-dependent quantum yields for the photodissocuation od acetone between 279 and 327.5 nm, Geophys. Res. Lett., 31, L06111, doi:10.1029/2003GL018793, 2004.

Broadgate, W. J., Liss, P. S., and Penkett, S. A.: Seasonal emissions of isoprene and other reactive hydrocarbon gases from the ocean, Geophys. Res. Lett., 24, 2675–2678, 1997.

Brühl, C., Pöschl, U., Crutzen, P. J., and Steil, B.: Acetone and PAN in the upper troposphere: impact on ozone production from aircraft emissions, Atmos. Environ., 34, 3931–3938, 2000.

Brunner, D., Staehelin, J., Rogers, H. L., Khler, M. O., Pyle, J. A., Hauglustaine, D., Jourdain, L., Berntsen, T. K., Gauss, M., Isaksen, I. S. A., Meijer, E., van Velthoven, P., Pitari, G., Mancini, E., Grewe, G., and Sausen, R.: An evaluation of the performance of chemistry transport models by comparison with research aircraft observations – Part 1: Concepts and overall model performance, Atmos. Chem. Phys., 3, 1609–1631, 2003, http://www.atmos-chem-phys.net/3/1609/2003/.

Cardelino, C. A. and Chameides, W. L.: Natural hydrocarbons, urbanization, and urban ozone, J. Geophys. Res., 95, 13971–13979, 1990.

Damian, V., Sandu, A., Damian, M., Potra, F., and Carmichael, G. R.: The kinetic preprocessor KPP – a software environment for solving chemical kinetics, Comput. Chem. Eng., 26, 1567–1579, 2002.

Damian-Iordache, V.: KPP – Chemistry Simulation Developement Environment, Master's thesis, University of Iowa, Iowa City, Iowa, USA, 1996.

Emmons, L. K., Hauglustaine, D. A., Müller, J.-F., Carroll, M. A., Brasseur, G. P., Brunner, D., Staehelin, J., Thouret, V., and Marenco, A.: Data composites of airborne observations of tropospheric ozone and its precursors, J. Geophys. Res., 105, 20497–20538, 2000.

Folberth, G. A., Hauglustaine, D. A., Lathiére, J., and Brocheton, F.: Interactive chemistry in the Laboratoire de Météorologie Dynamique general circulation model: model description and impact analysis of biogenic hydrocarbons on tropospheric chemistry, Atmos. Chem. Phys., 6, 2273–2319, 2006, http://www.atmos-chem-phys.net/6/2273/2006/.

Folkins, I. and Chatfield, R.: Impact of acetone on ozone production and OH in the upper

troposphere at high NO_x, J. Geophys. Res., 105, 11585–11599, 2000.

Friedrich, R. and Obermeier, A.: Anthropogenic emissions of volatile organic compounds, Academic, San Diego, California, USA, 2–38, 1999.

Gautrois, M., Brauers, T., Koppmann, R., Rohrer, F., Stein, O., and Rudolph, J.: Seasonal variability and trends of volatile organic compounds in the lower polar troposphere, J. Geophys. Res., 108, 4393, doi:10.1029/2002JD002765, 2003.

Goldan, P. D., Kuster, W., Fehsenfeld, F., and Montzka, S.: Hydrocarbon measurements in the southeastern United States: The Rural Oxidants in the Southern Environment (ROSE) program 1990, J. Geophys. Res., 100, 35945–35963, 1995.

Goldan, P. D., Parrish, D. D., Kuster, W. C., Trainer, M., McKeen, S., Holloway, J., Jobson, B., Sueper, D., and Fehsenfeld: Airborne measurements of isoprene,CO, and anthropogenic hydrocarbons and their implications, J. Geophys. Res., 105, 9091–9105, 2000.

Guenther, A., Geron, C., Pierce, T., Lamb, B., Harley, P., and Fall, R.: Natural emissions of non-methane volatile organic compounds, carbon monoxide, and oxides of nitrogen from North America, Atmos. Environ., 34, 2205–2230, 2000.

Gupta, M. L., Cicerone, R. J., Blake, D. R., Rowland, F. S., and Isaksen, I. S. A.: Global atmospheric distributions and source strengths of light hydrocarbons and tetrachloroethene, J. Geophys. Res., 103, 28219–28235, 1998.

Hagerman, L. M., Aneja, V. P., and Lonneman, W. A.: Characterization of non-methane hydrocarbons in the rural southeast United States, Atmos. Environ., 23, 4017–4038, 1997.

Houweling, S., Dentener, F., and Lelieveld, J.: The impact of non-methane hydrocarbon compounds on tropospheric photochemistry, J. Geophys. Res., 103, 10673–10696, 1998.

Jacob, D., Field, B., Jin, E., Bey, I., Li, Q., Logan, J., and Yantosca, R.: Atmospheric budget of acetone, J. Geophys. Res., 107, 4100, doi:10.1029/2001JD000 694, 2002.

Jaeglé, L., Jacob, D. J., Brune, W. H., and Wennberg, P. O.: Chemistry of HO_x radicals in the upper troposphere, Atmos. Environ., 35, 469–489, 2001.

Jeuken, A., Siegmund, P., Heijboer, L., Feichter, J., and Bengtsson, L.: On the potential assimilating meteorological analyses in a global model for the purpose of model validation, J. Geophys. Res., 101, 16939–16950, 1996.

Jobson, B. T., Wu, Z., Niki, H., and Barrie, L. A.: Seasonal trends of isoprene, alkanes, and acetylene at a remote boreal site in Canada, J. Geophys. Res., 99, 1589–1599, 1994.

Jöckel, P., Sander, R., Kerkweg, A., Tost, H., and Lelieveld, J.: Technical Note: The Modular Earth Submodel System (MESSy) – a new approach towards Earth System Modeling, At-

mos. Chem. Phys., 5, 433–444, 2005,
http://www.atmos-chem-phys.net/5/433/2005/.
Jöckel, P., Tost, H., Pozzer, A., Brühl, C., Buchholz, J., Ganzeveld, L., Hoor, P., Kerkweg, A., Lawrence, M. G., Sander, R., Steil, B., Stiller, G., Tanarhte, M., Taraborrelli, D., van Aardenne, J., and Lelieveld, J.: The atmospheric chemistry general circulation model ECHAM5/MESSy1: consistent simulation of ozone from the surface to the mesosphere, Atmos. Chem. Phys., 6, 5067–5104, 2006,
http://www.atmos-chem-phys.net/6/5067/2006/.
Kerkweg, A., Buchholz, J., Ganzeveld, L., Pozzer, A., Tost, H., and Jöckel, P.: Technical Note: An implementation of the dry removal processes DRY DEPosition and SEDImentation in the Modular Earth Submodel System (MESSy), Atmos. Chem. Phys., 6, 4617–4632, 2006,
http://www.atmos-chem-phys.net/6/4617/2006/.
Kerkweg, A., Sander, R., Tost, H., and Jöckel, P.: Technical note: Implementation of prescribed (OFFLEM), calculated (ONLEM), and pseudo-emissions (TNUDGE) of chemical species in the Modular Earth Submodel System (MESSy), Atmos. Chem. Phys., 6, 3603–3609, 2006,
http://www.atmos-chem-phys.net/6/3603/2006/.
Kerkweg, A., Jöckel, P., Pozzer, A., Tost, H., Sander, R., Schulz, M., Stier, P., Vignati, E., Wilson, J., and Lelieveld, J.: Consistent simulation of bromine chemistry from the marine boundary layer to the stratosphere – Part 1: Model description, sea salt aerosols and pH, Atmos. Chem. Phys., 8, 5899–5917, 2008a.
Kerkweg, A., Jöckel, P., Warwick, N., Gebhardt, S., Brenninkmeijer, C. A. M., and Lelieveld, J.: Consistent simulation of bromine chemistry from the marine boundary layer to the stratosphere – Part 2: Bromocarbons, Atmos. Chem. Phys., 8, 5919–5939, 2008,
http://www.atmos-chem-phys.net/8/5919/2008/.
Kesselmeier, J. and Staudt, M.: Biogenic Volatile Organic Compounds (VOC): An Overview on Emission, Physiology and Ecology, J. Atmos. Chem., 33, 23–88, 1999.
Lee, H. B., Munger, J., Steven, C., and Goldstein, A. H.: Anthropogenic emissions of non-methane hydrocarbons in the northeastern United Sates: Measured seasonal variations from 1992–1996 and 1999–2001, J. Geophys. Res., 111, D20307, doi:10.1029/2005JD006172, 2006.
Lelieveld, J., Brühl, C., Jöckel, P., Steil, B., Crutzen, P. J., Fischer, H., Giorgetta, M. A., Hoor, P., Lawrence, M. G., Sausen, R., and Tost, H.: Stratospheric dryness: model simulations and satellite observations, Atmos. Chem. Phys., 7, 1313–1332, 2007,

http://www.atmos-chem-phys.net/7/1313/2007/.
Lelieveld, J., Berresheim, H., Borrmann, S., et al.: Global Air Pollution Crossroads over the Mediterranean, Science, 298, 794–799, 2002.
Logan, J. A.: Tropospheric ozone: Seasonal behavior, trends, and anthropogenic influence, J. Geophys. Res., 90, 10463–10482, 1985.
McKeen, S. A., Gierczak, T., Burkholder, J. B., Wennberg, P. O., Hanisco, T. F., Keim, E. R., Gao, R.-S., Liu, S. C., Ravishankara, A. R., and Fahey, D. W.: The photochemistry of acetone in the upper troposphere: A source of odd-hydrogen radicals, Geophys. Res. Lett., 24, 3177–3180, 1997.
McLaren, R., Singleton, D. L., Lay, J. Y., Khouw, B., Singer, E., Wu, Z., and Niki, H.: Analysis of motor vehicle sources and their contribution to ambient hydrocarbon distributions at urban sites in Toronto during the Southern Ontario Oxidants Study, Atmos. Environ., 30, 2219–2232, 1996.
Middleton, P., Stockwell, W. R., and Carter, W. P. L.: Aggregation and analysis of volatile organic compound emissions for regional modeling, Atmos. Environ., 24A, 1107–1133, 1990.
Moxim, W. J., Levy, H., and Kasibhatla, P. S.: Simulated global tropospheric PAN: Its transport and impact on NO_x, J. Geophys. Res., 101, 12621–12638, 1996.
Müller, J.-F. and Brasseur, G.: IMAGES: A three-dimensional chemical transport model of the global troposphere, J. Geophys. Res., 100, 16445–16490, 1995.
Neeb, P.: Structure-Reactivity Based Estimation of the Rate Constants for Hydroxyl Radical Reactions with Hydrocarbons, J. Atmos. Chem., 35, 295–315, 2000.
Olivier, J. G. J., Bouwman, A. F., van der Maas, C. W. M., Berdowski, J. J. M., Veldt, C., Bloos, J. P. J., Visschedijk, A. J. J., Zandveld, P. Y. J., and Haverlag, J. L.: Description of EDGAR Version 2.0: A set of global inventories of greenhouse gases and ozone-depleting substances for all anthrophogenic and most natural sources on a per country $1^\circ \times 1^\circ$ grid, RIVM Rep. 771060002, Rijksinstituut, Bilthoven, The Netherlands, 1996.
Olivier, J. G. J., Bloos, J. P. J., Berdowski, J. J. M., Visschedijk, A. J. H., and Bouwman, A. F.: A 1990 global emission inventory of anthropogenic sources of carbon monoxide on $1^\circ \times 1^\circ$ developed in the framework of EDGAR/GEIA, Chemosphere, 1, 1–17, 1999.
Parrish, D., Stohl, A., Forster, C., Atlas, E., Blake, D., Goldan, P., Kuster, W. C., and de Gouw, J.: Effects of mixing on evoultion of hydrocarbon ratios in the troposphere, J. Geophys. Res., 112, D10S34, doi:10.1029/2006JD007583, 2007.
Plass-Dülmer, C., Koppmann, R., Ratte, M., and Rudolph, J.: Light non-methane hydrocarbons

in seawater, Global Biogeochem. Cy., 9, 79–100, 1995.
Poisson, N., Kanakidou, M., and Crutzen, P. J.: Impact of non-methane hydrocarbons on tropospheric chemistry and the oxidizing power of the global troposphere: 3-dimensional modelling results, J. Atmos. Chem., 36, 157–230, 2000.
Pollmann, J., Helmig, D., Hueber, J., Plass-Dülmer, C., and Tans, P.: Sampling,storage and analysis C_2-C_7 non-methane hydrocarbons from the US National Oceanic and Atmospheric Administration Cooperative Air Sampling Network glass flasks, J. Chromatogr. A, 1188, 75–87, 2008.
Pozzer, A., Jöckel, P., Tost, H., Sander, R., Ganzeveld, L., Kerkweg, A., and Lelieveld, J.: Simulating organic species with the global atmospheric chemistry general circulation model ECHAM5/MESSy1: a comparison of model results with observations, Atmos. Chem. Phys., 7, 2527–2550, 2007, http://www.atmos-chem-phys.net/7/2527/2007/.
Prather, M., McElroy, M., Wofsy, S., Russel, G., and Rind, D.: Chemistry of the Global Troposphere: Fluorocarbons as Tracers of Air Motion, J. Geophys. Res., 92, 6579–6613, 1987.
Raper, J., Kleb, M., Jacob, D., Davis, D., Newell, R., Fuelberg, H., Bendura, R., Hoell, J., and McNeal, R.: Pacific Exploratory Mission in the Tropical Pacific: PEM-Tropics B, March–April 1999, J. Geophys. Res., 106, 32401–32425, 2001a.
Raper, J. L., Kleb, M. M., Jacob, D. J., Davis, D. D., Newell, R. E., Fuelberg, H. E., Bendura, R. J., Hoell, J. M., and McNeal, R. J.: Pacific Exploratory Mission in the tropical Pacific: PEM-Tropics B, March–April 1999, J. Geophys. Res., 106, 32401–32425, 2001b.
Roberts, J. M., Jutte, R. S., Fehsenfeld, F. C., Albriton, D. L., and Sievers, R. E.: Measurements of anthropogenic hydrocarbon concentration ratios in the rural troposphere: Discrimination between background and urban sources, Atmos. Environ., 19, 1945–1950, 1985.
Roeckner, E., Brokopf, R., Esch, M., Giorgetta, M., Hagemann, S., Kornblueh, L., Manzini, E., Schlese, U., and Schulzweida, U.: Sensitivity of simulated climate to horizontal and vertical resolution in the ECHAM5 atmosphere model, J. Climate, 19, 3771–3791, 2006.
Roelofs, G.-J. and Lelieveld, J.: Tropospheric ozone simulation with a chemistry-general circulation model: Influence of higher hydrocarbon chemistry, J. Geophys. Res., 105, 22697–22712, 2000.
Rood, R. B.: Numerical advection algorithms and their role in atmospheric transport and chemistry models, Rev. Geophys., 25, 71–100, 1987.
Saito, T., Yokouchi, Y., and Kawamura, K.: Distribution of C_2-C_6 hydrocarbons over the western

north Pacific and eastern Indian Ocean, Atmos. Environ., 34, 4373–4381, 2000.
Sander, R., Kerkweg, A., Jöckel, P., and Lelieveld, J.: Technical note: The new comprehensive atmospheric chemistry module MECCA, Atmos. Chem. Phys., 5, 445–450, 2005, http://www.atmos-chem-phys.net/5/445/2005/.
Saunders, S. M., Jenkin, M. E., Derwent, R. G., and Pilling, M. J.: Protocol for the development of the Master Chemical Mechanism, MCM v3 (Part A): tropospheric degradation of non-aromatic volatile organic compounds, Atmos. Chem. Phys., 3, 161–180, 2003, http://www.atmos-chem-phys.net/3/161/2003/.
Schultz, M. G., Jacob, D. J., Wang, Y., Logan, J. A., Atlas, E., Blake, D. R., Blake, N. J., Bradshaw, J. D., Browell, E. V., Fenn, M. A., Flocke, F., Gregorz, G. L., Heikes, B. G., Sachse, G. W., Sandholm, S. T., Shetter, R. E., Singh, H. B., and Talbot, R. W.: On the origin of tropospheric ozone and NO_x over the tropical South Pacific, J. Geophys. Res., 104, 5829–5844, 1999.
Schultz, M. G., Jacob, D. J., Bradshaw, J. D., Sandholm, S. T., Dibb, J. E., Talbot, R. W., and Singh, H. B.: Chemical NO_x Budget in the Upper Troposphere over the Tropical South Pacific, J. Geophys. Res., 105, 6669–6679, 2000.
Seinfeld, J. H. and Pandis, S.: Atmospheric Chemistry and Physics: From Air Pollution to Climate Change, Wiley-Interscience, 1997.
Sharma, U. K., Kajii, Y., and Akimoto, H.: Seasonal variation of C_2-C_6 NMHCs at Happo, a remote site in Japan, Atmos. Environ., 34, 4447–4458, 2000.
Singh, H. B. and Zimmermann, P.: Atmospheric distribution and sources of nonmethane hydrocarbons, John Wiley, New York, USA, 1992.
Singh, H. B., O'Hara, D., Herlth, D., Sachse, W., Blake, D. R., Bradshaw, J. D., Kanakidou, M., and Crutzen, P. J.: Acetone in the atmosphere: Distribution, source, and sinks, J. Geophys. Res., 99, 1805–1819, 1994.
Singh, H. B., Kanakidou, M., Crutzen, P. J., and Jacob, D. J.: High concentrations and photochemical fate of oxygenated hydrocarbons in the global troposphere, Nature, 378, 50–54, 1995.
Singh, H. B., Chen, Y., Staudt, A. C., Jacob, D. J., Blake, D. R., Heikes, B. G., and Snow, J.: Evidence from the Pacific troposphere for large global sources of oxygenated organic compounds, Nature, 410, 1078–1081, 2001.
Singh, H. B., Tabazadeh, A., Evans, M. J., Field, B. D., Jacob, D. J., Sachse, G., Crawford, J. H., Shetter, R., and Brune, W. H.: Oxygenated volatile organic chemicals in the oceans: Infer-

ences and implications based on atmospheric observations and air-sea exchange models, Geophys. Res. Lett., 30, 1862, doi:10.1029/2003GL017933, 2003.
Singh, H. B., Salas, L. J., Ridley, B. A., et al.: Relationship between peroxyacetyl nitrate (PAN) and nitrogen oxides in the clean troposphere, Nature, 318, 347–349, 1985.
Spivakovsky, C. M., Logan, J. A., Montzka, S. A., Balkanski, Y. J., Foreman-Fowler, M., Jones, D. B. A., Horowitz, L. W., Fusco, A. C., Brenninkmeijer, C. A. M., Prather, M. J., Wofsy, S. C., and McElroy, M. B.: Three-dimensional climatological distribution of tropospheric OH: Update and evaluation, J. Geophys. Res., 105, 8931–8980, 2000.
Swanson, A., Blake, N., Atlas, E., Flocke, F., Blake, D. R., and Sherwood, F.: Seasonal variation of C_2-C_4 nonmethane hydrocarbons and C_1-C_4 alkyl nitrates at the Summit research station in Greenland, J. Geophys. Res., 108, D24065, doi:10.1129/2001JD001445, 2003.
Tost, H., Jöckel, P., Kerkweg, A., Sander, R., and Lelieveld, J.: Technical note: A new comprehensive SCAVenging submodel for global atmospheric chemistry modelling, Atmos. Chem. Phys., 6, 565–574, 2006, http://www.atmos-chem-phys.net/6/565/2006/.
Traub, M., Fischer, H., de Reus, M., Kormann, R., Heland, H., Ziereis, H., Schlager, H., Holzinger, R., Williams, J., Warneke, C., de Gouw, J., and Lelieveld, J.: Chemical characteristics assigned to trajectory clusters during the MINOS campaign, Atmos. Chem. Phys., 3, 459–468, 2003, http://www.atmos-chem-phys.net/3/459/2003/.
Tyndall, G. S., Staffelbach, T. A., Orlando, J. J., and Calvert, J. G.: Rate coefficients for the reactions of OH radicals with methylglyoxal and acetaldehyde, Int. J. Chem. Kinet., 27, 1009–1020, 1995.
Tyndall, G. S., Orlando, J. J., Wallington, T. J., Hurley, M. D., Goto, M., and Kawasaki, M.: Mechanism of the reaction of OH radicals with acetone and acetaldehyde at 251 and 296 K, Phys. Chem. Chem. Phys., 4, 2189–2193, 2002.
van Aardenne, J., Dentener, F., Olivier, J., Peters, J., and Ganzeveld, L.: The EDGAR 3.2 Fast Track 2000 dataset (32FT2000), online: http://www.mnp.nl/edgar/model/v32ft2000edgar/docv32ft2000/, 2005.
van Aardenne, J. A., Dentener, F. J., Olivier, J. G. J., Klein Goldewijk, C. G. M., and Lelieveld, J.: A 1°×1° resolution data set of historical anthropogenic trace gas emissions for the period 1890–1990, Global Biogeochem. Cy., 15, 909–928, 2001.
von Kuhlmann, R., Lawrence, M. G., Crutzen, P. J., and Rasch, P. J.: A Model for Studies of

Tropospheric Ozone and Non-Methane Hydrocarbons: Model Evaluation of Ozone Related Species, J. Geophys. Res., 108, 4729, doi:10.1029/2002JD003348, 2003.
Wennberg, P. O., Hanisco, T. F., Jaeglé, L., Jacob, D., Hintsa, E. J., Lanzendorf, E. J., Anderson, J. G., Gao, R.-S., Keim, E. R., Donnelly, S. G., Negro, L. A. D., Fahey, D. W., McKeen, S. A., Salawitch, R. J., Webster, C. R., May, R. D., Herman, R. L., Proffitt, M. H., Margitan, J. J., Atlas, E. L., Schauffler, S. M., Flocke, F., McElroy, C. T., and Bui, T. P.: Hydrogen radicals, nitrogen radicals, and the production of O_3 in the upper troposphere, Science, 279, 49–53, 1998.
World Meteorological Organization, W.: A WMO/GAW expert workshop on global long-term measurements of volatile organic compounds (VOCs), Tech. rep., WMO Rep.171, Geneva, Switzerland, 2007.

Table 1. Total emissions of different trace gases in the EMAC simulation (this study) compared to previous studies.

	emissions (Tg/yr)			
Olivier et al. (1996)	Jacob et al. (2002)	Gautrois et al. (2003)	this study	
C_3H_8	7.6	13.46	18.4	12.0
n-C_4H_{10}	14.1	–	22.7	9.87
l-C_4H_{10}		4.2		4.23
n-C_5H_{12}	12.4	–	8.2	4.34
l-C_5H_{12}		7.3	–	8.06

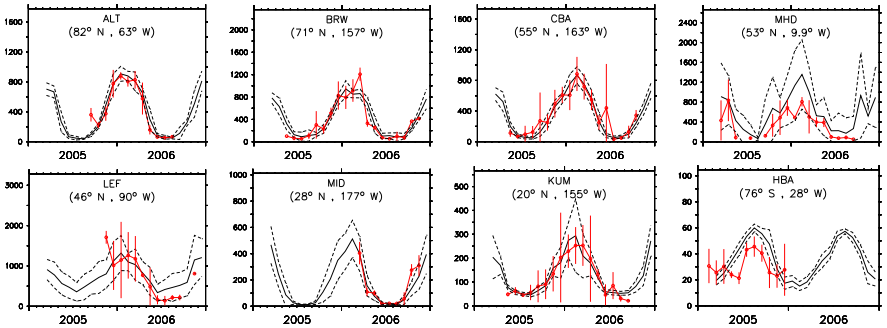

Fig. 1. Comparison of simulated and observed C_3H_8 mixing ratios in pmol/mol for some selected locations (ordered by latitude). The red lines and the bars represent the monthly averages and standard deviations (with respect to time) of the measurements. No instrumental error was included in this standard deviation. The simulated monthly averages are indicated by the black lines and the corresponding simulated standard deviations (with respect to time) by the dashed lines. The three letters at the center of each plot denote the station code (see http://www.esrl.noaa.gov/gmd/ccgg/flask.html).

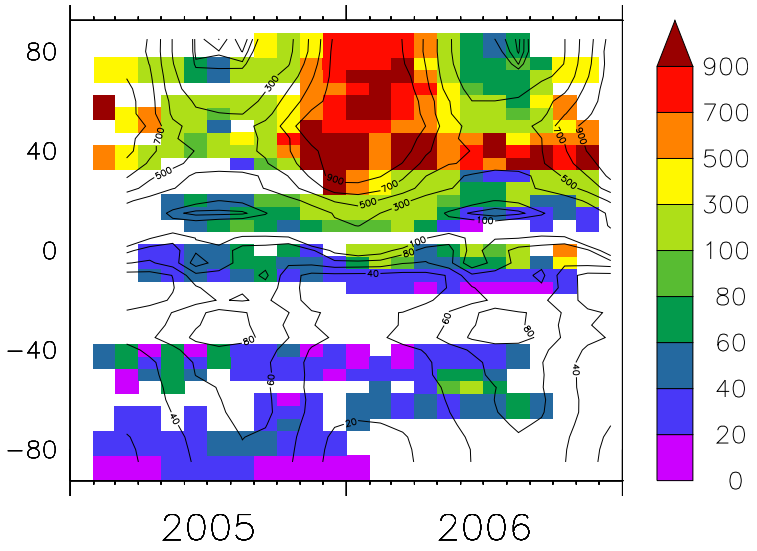

Fig. 2. Seasonal cycle and meridional distribution of propane (C_3H_8). The color code denotes the mixing ratios in pmol/mol, calculated as a zonal average of the measurements available in the NOAA/CMDL dataset. The superimposed contour lines denote the zonal averages of the model results.

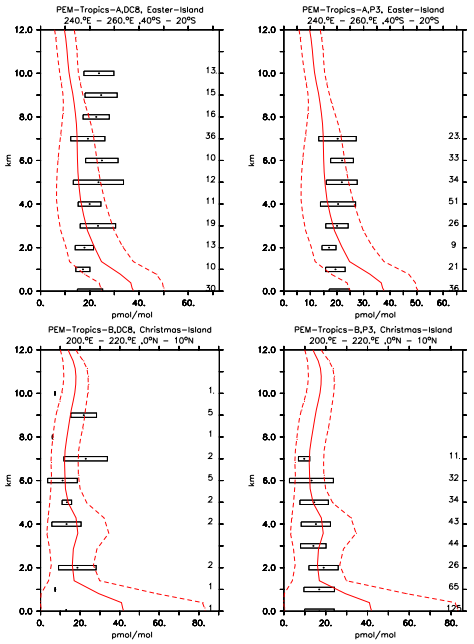

Fig. 3. Vertical profiles of C_3H_8 (in pmol/mol) for some selected campaigns from Emmons et al. (2000). The PEM-Tropics-A campaign has been performed during August–October 1996, while PEM-Tropics-B during March and April 1999. Asterisks and boxes represent the average and the standard deviation (with respect to space and time) of the measurements in the region, respectively. The simulated average is indicated by the red line and the corresponding simulated standard deviation with respect to time and space by the dashed lines. On the right axis the numbers of measurements are listed.

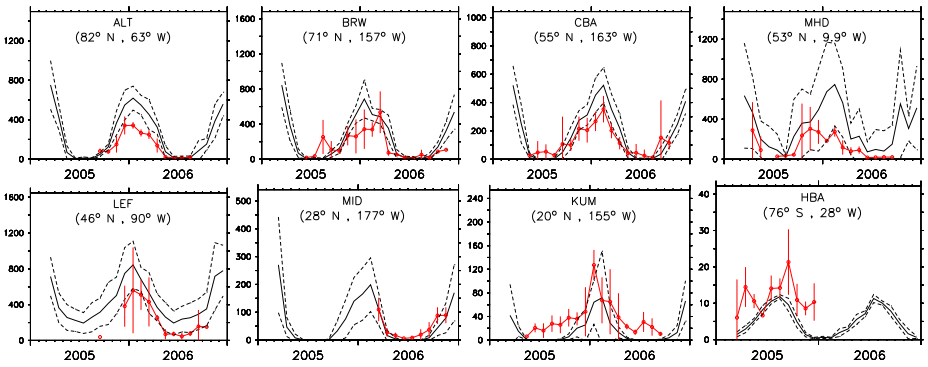

Fig. 4. As Fig. 1 for C_4H_{10}.

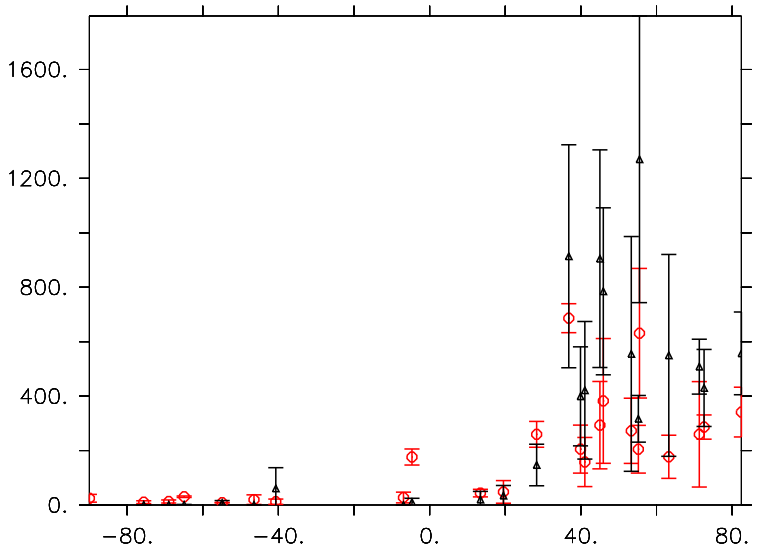

Fig. 5. C_4H_{10} simulation and observations (December 2005) in pmol/mol. The red circles represent the observation and the black triangles the model results. The red and black bars represent the standard deviation (variability) of the observation and model, respectively. The model was sampled at the location of the observation sites.

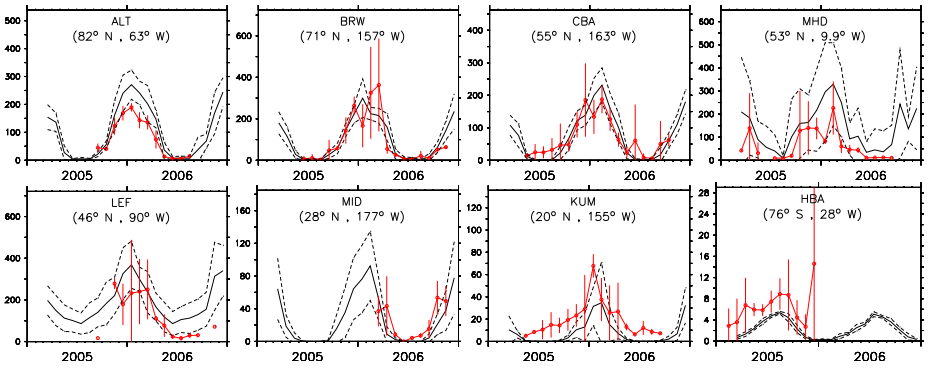

Fig. 6. As Fig. 1 for l-C_4H_{10}.

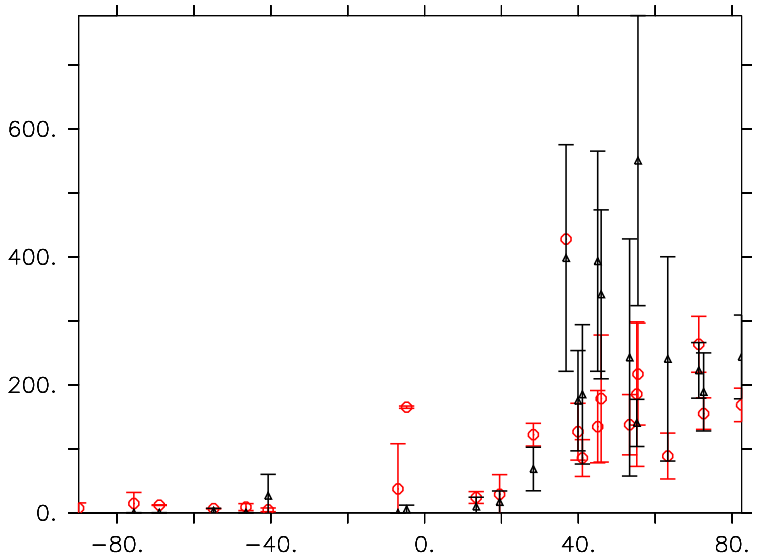

Fig. 7. As Fig. 5 for l-C_4H_{10}

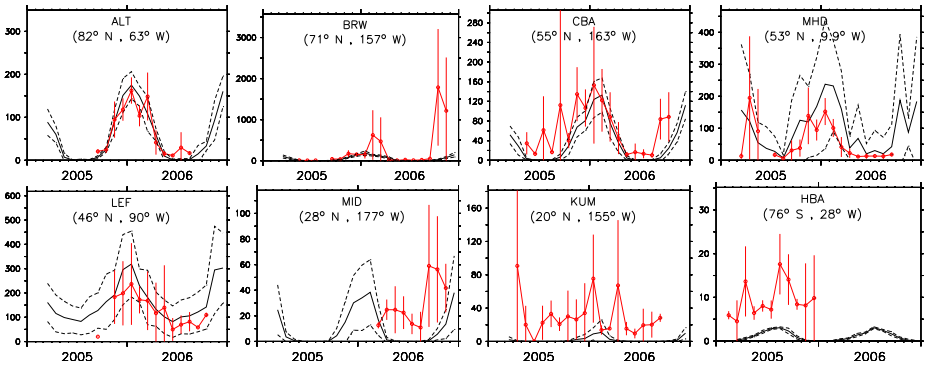

Fig. 8. As Fig. 1 for C_5H_{12}.

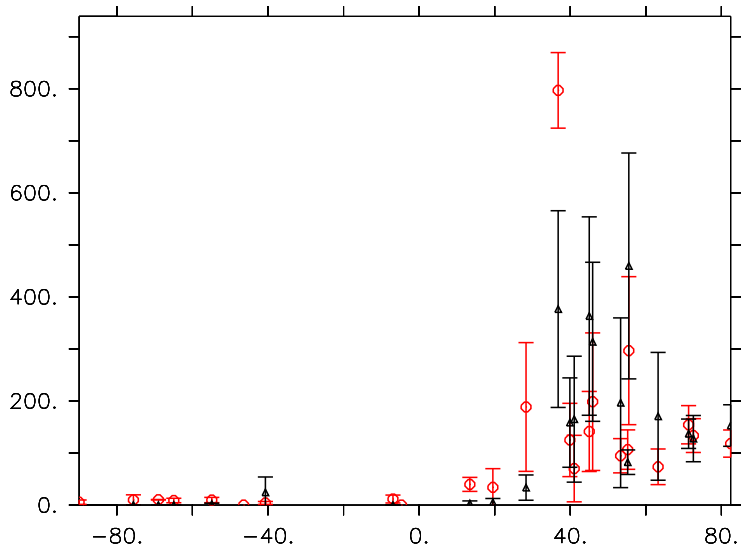

Fig. 9. As Fig. 5 for C_5H_{12}.

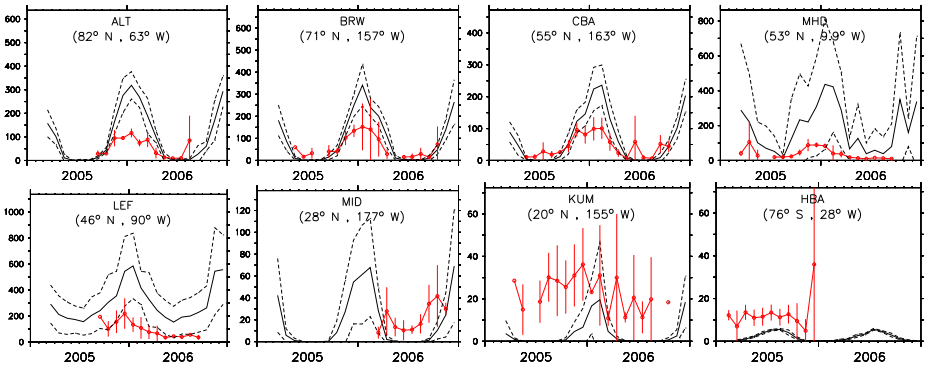

Fig. 10. As Fig. 1 for l-C_5H_{12}.

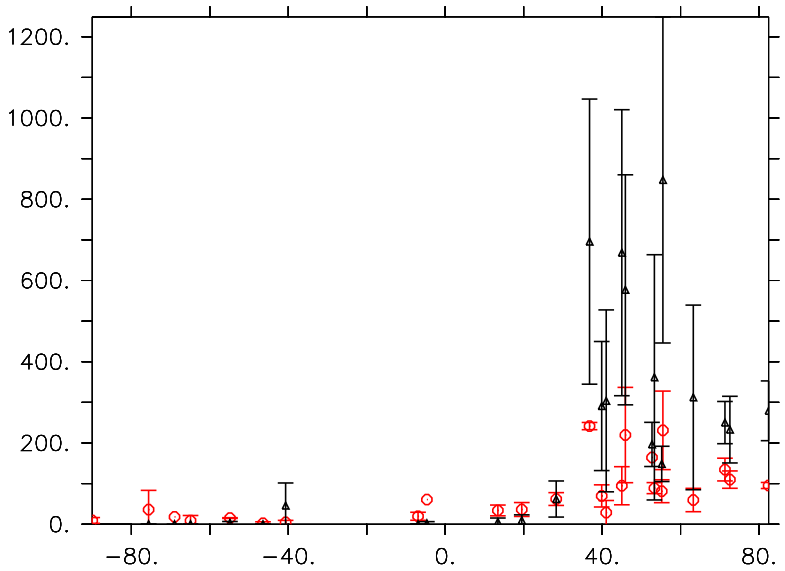

Fig. 11. As Fig. 5 for l-C_5H_{12}.

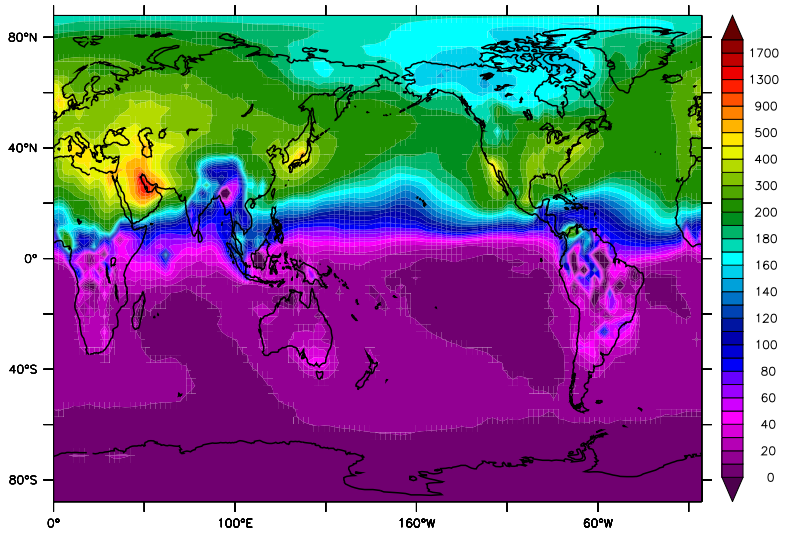

Fig. 12. Difference between the simulated annual average surface mixing ratio of CH_3COCH_3 from this study and the simulation S1, in pmol/mol.

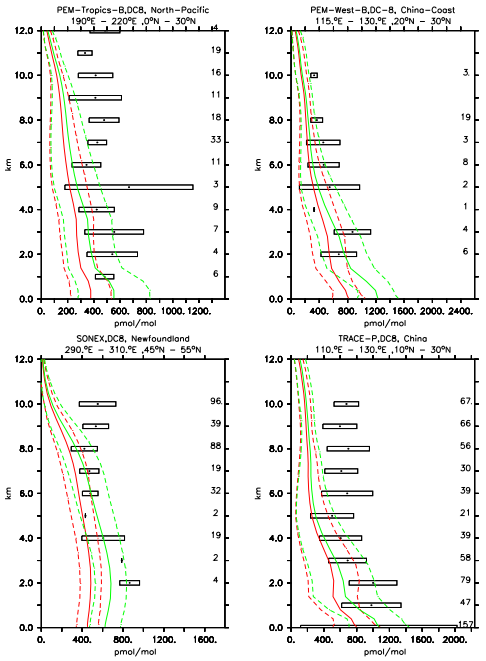

Fig. 13. Vertical profiles of CH_3COCH_3 (in pmol/mol). Symbols and lines as in Fig. 3. The red lines represent the simulation S1, the green lines the simulation from this study. The PEM-Tropics-B, PEM-West-B, SONEX and TRACE-P campaign took place in March–April 1999, February–March 1994, October–November 1997 and February–April 2001, respectively.